ORIGINAL ARTICLE

gebiology WILEY

Desert breath—How fog promotes a novel type of soil biocenosis, forming the coastal Atacama Desert's living skin

Patrick Jung[1] 🆔 | Karen Baumann[2] | Lukas W. Lehnert[3] | Elena Samolov[4] | Sebastian Achilles[5] | Michael Schermer[1] | Luise M. Wraase[6] | Kai-Uwe Eckhardt[2] | Maaike Y. Bader[6] 🆔 | Peter Leinweber[2] | Ulf Karsten[4] 🆔 | Jörg Bendix[5] 🆔 | Burkhard Büdel[1]

[1]Plant Ecology and Systematics, University of Kaiserslautern, Kaiserslautern, Germany

[2]Faculty of Agricultural and Environmental Science, Soil Science, University of Rostock, Rostock, Germany

[3]Department of Geography, Ludwig-Maximilians-University, Munich, Germany

[4]Institute of Biological Sciences, Applied Ecology and Phycology, University of Rostock, Rostock, Germany

[5]Faculty of Geography, Laboratory for Climatology and Remote Sensing, Philipps-University of Marburg, Marburg, Germany

[6]Faculty of Geography, Ecological Plant Geography, Philipps-University of Marburg, Marburg, Germany

Correspondence
Patrick Jung, Plant Ecology & Systematics, TU Kaiserslautern, Erwin-Schrödinger Straße 13, 67655 Kaiserslautern, Germany.
Email: Patrick_jung90@web.de

Funding information
We appreciated funding of the priority program EarthShape ("Earth Surface Shaping by Biota") by the German Research Foundation (BE1780/44-1, KA899/32-1, BU666/19-1, LE903/14-1).

Abstract

The Atacama Desert is the driest non-polar desert on Earth, presenting precarious conditions for biological activity. In the arid coastal belt, life is restricted to areas with fog events that cause almost daily wet–dry cycles. In such an area, we discovered a hitherto unknown and unique ground covering biocenosis dominated by lichens, fungi, and algae attached to grit-sized (~6 mm) quartz and granitoid stones. Comparable biocenosis forming a kind of a layer on top of soil and rock surfaces in general is summarized as cryptogamic ground covers (CGC) in literature. In contrast to known CGC from arid environments to which frequent cyclic wetting events are lethal, in the Atacama Desert every fog event is answered by photosynthetic activity of the soil community and thus considered as the desert's breath. Photosynthesis of the new CGC type is activated by the lowest amount of water known for such a community worldwide thus enabling the unique biocenosis to fulfill a variety of ecosystem services. In a considerable portion of the coastal Atacama Desert, it protects the soil from sporadically occurring splash erosion and contributes to the accumulation of soil carbon and nitrogen as well as soil formation through bio-weathering. The structure and function of the new CGC type are discussed, and we suggest the name *grit–crust*. We conclude that this type of CGC can be expected in all non-polar fog deserts of the world and may resemble the cryptogam communities that shaped ancient Earth. It may thus represent a relevant player in current and ancient biogeochemical cycling.

1 | INTRODUCTION

The Atacama Desert is one of the driest places in the world and occupies more than 120,000 km[2] (Rundel, Villagra, Dillon, Roig-Juñent, & Debandi, 2007). Here, life is challenged by high solar radiation, strong wind erosion, and severely limited access to water. Annual rainfall is very low and very variable, with many years without any rainfall (Hartley, Chong, Houston, & Mather, 2005; McKay et al., 2003). Such low water availability means that living organisms approach the limits of their existence. In fact, the biomass of soil microbiota of some parts in the arid zone of the Atacama Desert is one or two orders of magnitude lower than in any other dryland on Earth

(Drees et al., 2006; Navarro-Gonzales et al., 2003). Precipitation levels in these dry inland zones allow the establishment mainly of cyanobacteria that were found, for example, under translucent quartz stones and are known as lithic communities (stone-inhabiting communities including hypoliths and endoliths; Warren-Rhodes et al., 2006). Different types of cryptogamic organizations such as biological soil crusts (hereafter referred to as biocrusts), which are an edaphic biocenosis (community of organisms that interact with each other in a soil-like habitat) of cyanobacteria, algae, lichens, bryophytes, heterotrophic bacteria, archaea, and fungi living in the top soil layers (Belnap & Gardner, 1993), have only recently been reported to occur very locally in the Coastal Range of the Atacama Desert, in areas that are affected by fog (Baumann et al., 2018; Bernhard et al., 2018; Lehnert, Jung, Obermeier, Büdel, & Bendix, 2018a; Wang, Michalski, Luo, & Caffee, 2017).

Such cryptogamic ground covers (CGC; Elbert et al., 2012) are estimated to occur on about 12% of the Earth´s terrestrial surface, thus they are one of the most abundant and most productive microbial communities (Rodriguez-Caballero et al., 2018; Weber, Büdel, & Belnap, 2016). As "ecosystem-engineers" (Bowker, Mau, Maestre, Escolar, & Castillo-Monroy, 2011), CGCs often form surface layers that provide important ecosystem services that can be categorized as supporting services, for example, primary production and soil formation via bio-weathering or regulating services such as erosion prevention or influences on biogeochemical cycles. For example, they have an estimated contribution of nearly half of the global terrestrial biological N fixation and 7% of the net primary production of terrestrial vegetation (Elbert et al., 2012). They may also contribute importantly to global C cycles. Estimates of global C sources and sinks are still imbalanced (Quéré et al., 2018) with suspected sink functions of drylands (Evans et al., 2014; Ma, Liu, Tang, Lan, & Li, 2014) which are, however, not well quantified due to a significant lack of studies (Maestre et al., 2013). As the occurrence of CGCs is predominantly expressed in drylands (Weber et al., 2016), the ecosystem services of these areas may be consistently underestimated. In the Namib Desert, for example, biological activity of a CGC dominated by lichens is known to follow wet–dry cycles which are caused by fog, dew, and seasonal rainfall, therewith providing $16 \text{ g C m}^{-2} \text{ yr}^{-1}$ to the soil on a large scale (Lange, Meyer, Zellner, & Heber, 1994).

Despite significant advances in our understanding of the role of CGCs in deserts across the world, the questions about the extent of these biocoenoses or how they influence ecosystems remain unanswered. During explorations in the National Park Pan de Azúcar of the southern Atacama Desert, we discovered extended blackish patterns paving the ground which unlike the inorganic mineral crusts called *desert varnish* that are known from deserts worldwide (Selby, 1977), turned out to be caused by an hitherto unknown CGC type occurring at a large landscape scale.

In this article, we describe this new and unique type of CGC in the fog oasis of the Atacama Desert and address several hypotheses concerning its structure and function. We hypothesized that (a) these patterns of blackish and whitish soil areas were caused by variation in the density and composition of the cryptogamic cover,

(b) this cryptogamic cover was dominated by green-algal lichens (chlorolichens), free-living green algae, and cyanobacteria, because water availability is limited and thus only less water demanding cryptogam groups can thrive there, and (c) that this variation in biological cover was correlated with variation in geochemical soil properties. Additionally, we discuss the ecosystem services provided by the CGC organisms and relate this to the potential role of similar cryptogamic covers in ancient Earth and present-day biogeochemical processes.

2 | METHODS

2.1 | Study site

Pan de Azúcar National Park is located between 25°53′ to 26°15′S and 70°29′ to 70°40′W along the coast of Chile and is characterized by an arid climate (Baumann et al., 2018; Lehnert, Thies, et al., 2018b). A narrow pediment close to the coast is followed by a steep escarpment reaching elevations up to 850 m a. s. l. After the ridge of the escarpment, the terrain descends slightly to elevations between 400 and 700 m a. s. l. toward inland. This study was conducted within a strip of 2.5 km on top of the escarpment along the Pacific coast (Lat: 25.96636111°S, Long: 70.61521111°W). In this zone, quartz- and granitoid grit-sized (0.6 mm) stones paved the desert surface and abundant blackish patterns were observed.

2.2 | Remote sensing

Along the coastline, five transects were selected from the first ridge toward the hinterland. Areal images of each transect were acquired using drones equipped with standard RGB-cameras. Position and elevation of ground reference points were recorded prior to the flights using a differential GPS in post-processing mode. Spatial resolutions of the images varied between 1.8 cm and 3.5 cm depending on the flight height above the terrain. The total area covered by aerial images was 206.5 ha. RGB images were processed using AgiSoft PhotoScan (Riano, Chuvieco, Salas, & Aguado, 2003). To derive mosaics covering the entire flight path, the single images were stitched together, and digital surface models were calculated.

The mosaics were topographically corrected calculating the illumination at acquisition time and applying the method according to Minnaert (Vermote, Tanre, Deuze, Herman, & Morcette, 1997). Training areas in each image for classes "vegetation," "biocrust," and "bare soil" were defined using field observation data and the high-resolution drone images. Afterward, maximum likelihood classifications were performed using the red, green, and blue bands of the topographically corrected mosaics.

To provide estimates of CGCs over larger areas, a cloud-free satellite scene from Landsat 8 was used. The level-2 data were radiometrically, atmospherically, and topographically corrected to ground albedo values. For the radiometric correction, the standard correction values provided with the metadata were applied. For the atmospheric correction, an enhanced version of the 6S-code was applied which proved to perform superior to the original one in areas with

rugged terrain (Curatola Fernández et al., 2015) . The topographic correction method according to Minnaert was applied to the atmospherically corrected ground albedo values using the Aster digital elevation model.

The maximum likelihood classifications of the aerial images were used as reference for a cover classification of the Landsat 8 scene. For each Landsat 8 pixel, the percentage of the collocated aerial image pixels covered by the biocrust was calculated giving estimates on cover of the new biocrust. These estimates were used as response variables in random forest regression models. As predictors, the atmospherically and topographically corrected Landsat 8 albedo values were used. Since the occurrence of the new CGC strongly depends on fog water fluxes, the mean values of liquid water path of low stratus clouds and fog as derived by a novel fog retrieval with 30 m spatial resolution were used as an additional predictor in the random forest models (Lehnert, Thies, & Bendix (unpublished data). Tuning and validation were performed based on a 10-fold cross-validation repeated five times. The root–mean–square error of the CGC estimates was 4.00% with an R^2 value of 0.88. The final model was applied to the entire area of the Pan de Azúcar National Park and its surrounding desert. The occurrence (presence/absence) of the grit–crust outside of the drone transects was successfully validated at ten additional sites shown as red dots in Figure 1d.

2.3 | Climatic data

In order to determine climate conditions in the area of the CGC (Lat: 25.96636111°S, Long: 70.61521111°W; 2.5 km distance from the Pacific coast), an automatic weather station (AWS grit) was installed which has delivered data between July 2017 and March 2018 in 5-min intervals. The AWS is equipped with standard sensors measuring wind speed and direction, air and soil temperature, relative humidity, and a surface temperature sensor pointing at the biocrust. Fog and dew water flues are determined using a cylindrical ("harp"-type) fog collector and a dew balance on the ground, with the biocrust pieces glued on. Additionally, rainfall is measured at another AWS (AWS main, Lat: 25.984372°S, Lon: 70.61528°W) directly at the Pacific coast. The setup, calibration, and first results are described in Lehnert, Thies, et al., 2018b.

2.4 | Sampling

To characterize the blackish and whitish areas chemically, physiologically, and taxonomically, five substrate replicates of the blackish and whitish patterns each were taken from random positions in close vicinity to the AWS. For the soil analysis and chlorophyll determination, five replicates were used and for ecophysiological experiments and species identification, ten replicates were used. Samples were taken from the top first cm by pressing a 9 cm diameter sterile petri dish into the substrate. All samples were stored in a dry state and kept in the dark at room temperature for one week until the investigations.

2.5 | Substrate parameters and chlorophyll contents

From five replicates, each of whitish and blackish pattern substrate, pH (H$_2$O, 1:2.5 w:v) and electrical conductivity (EC, 1:5 w:v) were determined by standard procedures (Blume, Stahr, & Leinweber, 2010). For total element analyses, air-dry substrate was ground to <0.5 mm. Total C, N, and S (C$_t$, N$_t$, S$_t$) were measured using a Vario EL elemental analyzer (Elementar Analysensysteme). Inorganic carbon (C$_{inorg}$) was analyzed by the Scheibler method (DIN ISO 10693), and organic carbon (C$_{org}$) was calculated by difference (C$_t$ – C$_{inorg}$). Total Al, Ca, Fe, K, Mg, Mn, P, and Zn were extracted from 0.5 g substrate by microwave-assisted digestion with aqua regia solution (3:1 hydrochloric acid:nitric acid) (Chen & Ma, 2001 ISO standard 11466) and subsequent determination by ion-coupled plasma—optical emission spectroscopy (ICP-OES).

Chlorophyll was extracted from five samples of the whitish pattern as well as five samples of the blackish one using a DMSO method as described in (Ronen & Galun, 1984) and calculated to area.

2.6 | Pyrolysis field ionization mass spectrometry (Py-FIMS)

To gain in depth information on the organic matter potentially provided by the CGC during soil formation, pyrolysis field ionization mass spectrometry (Py-FIMS) was applied to three replicates containing 0.5 mg of the CGC community which were scraped off the grit stones. Samples were degraded by pyrolysis in the ion source (emitter: 4.7 kV, counter electrode −5.5 kV) of a double-focusing Finnigan MAT 95. The samples were heated in a vacuum of 10^{-4} Pa from 50°C to 650°C, in temperature steps of 10°C over a time period of 15 min. Between magnetic scans, the emitter was flash heated to avoid residues of pyrolysis products. Sixty spectra were recorded for the mass range 15–900 m/z. At each scan, the mass range of m/z 15–900 was recorded and the absolute and relative ion intensities of nine classes of chemical compounds were calculated by summation of the ion intensities of indicator signals to obtain thermograms of their volatilization (Schulten & Leinweber, 1999). The compound classes were: carbohydrates with pentose and hexose subunits (CHYDR), phenols and lignin monomers (PHLM), lignin dimers (LDIM), lipids, alkanes, alkenes, bound fatty acids, alkyl monoesters and sterols (LIPSTERO), alkylaromatics (ALKYL), mainly heterocyclic N-containing compounds (NCOMP), peptides (PEPTI), suberin (SUBR), and free fatty acids (FATTY). Single magnetic scans were combined to obtain one thermogram of total ion intensity (TII) and a summed Py-FI mass spectrum. All Py-FIMS data were normalized per mg sample, and an average value for the CGC community was calculated from the three field replicates. Thermostability of the sample was calculated by dividing the sum of all ion intensities from 50 to 400°C by the sum of all ion intensities from 50 to 650°C.

2.7 | Ecophysiology

CO$_2$ exchange measurements were conducted under controlled laboratory conditions using a minicuvette system (CMS400, Walz Company, Effeltrich, Germany). The response of gross
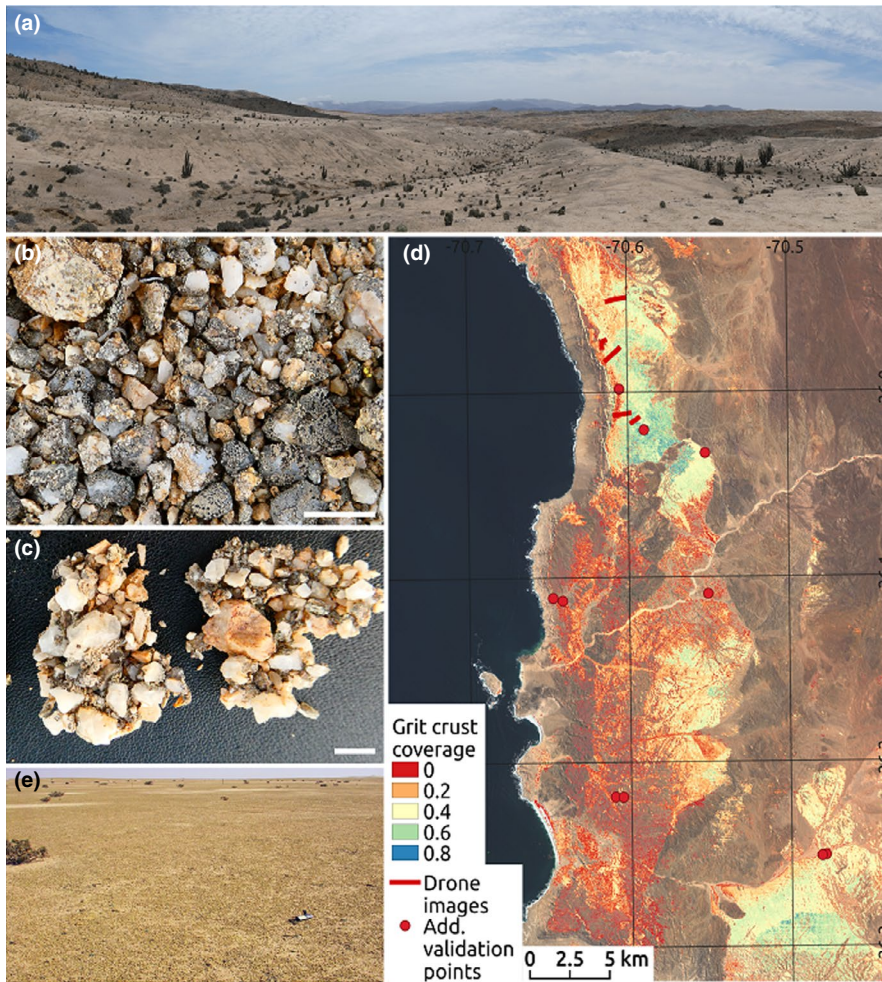
FIGURE 1 Grit-crust ecosystems. (a) Blackish and whitish patterns caused by the newly discovered 'grit-crust' biocrust in the landscape of Las Lomitas in the National Park Pan de Azúcar, South Atacama Desert, Chile. (b) Close up of blackish appearing grits covered by various lichens and concatenated grit-crust (c), each with a scale bar of 1 cm. (d) Map of the estimated coverage of the grit-crust at National Park Pan de Azúcar derived from remote sensing. Red lines indicate the location of the drone transects and red dots are additional points, where occurrence of grit-crust was validated in the field (e), Biocrusts within fog zones of the Namib Desert

photosynthesis (net photosynthesis (NP) + dark respiration (DR)) related to water content was determined for five samples. Complete desiccation cycles (from water-saturated thalli to air-dry) were measured at 800 μmol photons/m^2 s^{-1}, ambient CO_2, and at temperatures of 5°C, 10°C, 15°C, and 20°C. Samples were weighed before each measurement and the water content was calculated as mm precipitation equivalent, following the determination of the samples dry weights after a three-day drying period at 65°C in a drying oven (Heraeus Instruments T6P, Thermo Fisher Scientific Inc.). To obtain the NP response to light, fully hydrated samples were exposed to stepwise increasing photosynthetically active radiation (PAR) from 0 to 2,000 μmol photons/m^2 s^{-1} at optimal temperature (15°C) and ambient CO_2 concentration. The light cycle (about 45 min duration) was repeated until the samples were completely dry (after 5 hr). Light saturation point (LSP) was defined as the photosynthetic photon flux density at 90% of maximum NP. The CO_2 exchange of the samples was related to surface area.

2.8 | Microscopy and cultures

To study the taxonomic composition of the CGC, we used several methods, depending on the taxa. Direct microscopy of the blackish and whitish samples was applied to address the morphological

diversity of pro- and eukaryotic algae. An aliquot of a CGC sample, prepared by washing loose organisms off the grit stones, was collected in a drop of water and examined under a stereoscope binocular (2000-C, Zeiss, Germany). The samples were investigated with a light microscope (Axioskop, Zeiss, Germany with DIC optics) under 630 magnification and oil immersion. Additionally, a culture-based approach was applied to all biocrust samples as described in (Baumann et al., 2018).

After at least four weeks, green algae were transferred to BBM agar plates (Bischoff & Bold, 1963) and cyanobacteria to BG11 agar plates (Stanier, Kunisawa, Mandel, & Cohen-Bazire, 1971), using a sterile needle. This was repeated until unialgal cultures were established. Morphology of the phototrophs was studied by light microscopy as explained above. Based on the relevant morphological characters, eukaryotic algae and cyanobacteria were identified to the genus, and if possible, to the species level based on the most recent literature as described by Baumann et al. (2018).

Lichens were identified by carefully removing them from a single grit in a hydrated state with a sterile needle and transferred to a freezing microtome. Thin sections of 25 μm thickness were prepared and transferred to a drop of water on an object slide. Fully hydrated lichens covering grit stones were visualized with the same stereoscope binocular.

For electron microscopy, a low-temperature scanning electron microscope (Supra 55VP; Carl Zeiss, Oberkochen, Germany) was used to study fully hydrated *Lichenothelia* sp. The samples were frozen in liquid nitrogen slush (K1250X Cryogenic preparation system, Quorum technologies) and mounted on special brass trays. After sublimation for 30 min at −80°C, samples were sputter-coated with gold–palladium and viewed at a temperature of −130°C and 5 kV accelerator voltage.

Various colonized grit stones were embedded in water-free resin and cut into blocks after drying and hardening. The blocks were carefully ground down to a thickness of 30 μm and mounted between a glass objective slide and a cover slide. These thin sections were visualized with a epifluorescence microscope (Axioskop; HBO 50; Zeiss) as described above by exciting the autofluorescence of the mycobiont and the photobionts (blue–violet 395–440 nm excitatory filter; 460 nm chromatic beam splitter; 470 nm barrier filter).

2.9 | Statistics

Shapiro–Wilk test and *F* test revealed that the distribution of substrate and chlorophyll data was not always normal, and variances were not always homogeneous. Hence, Wilcoxon–Mann–Whitney *U* test was used to determine significant differences of the substrate parameters between whitish and blackish pattern. All statistical analyses were performed using R version 3.4.3 (R Core Team, 2017). Unless otherwise noted significant differences refer to $p \leq .05$.

3 | RESULTS

3.1 | Description of the microhabitat and biocenosis

The habitat of the newly detected CGC was located 2.5 km off the Pacific coast in the local fog oasis "Las Lomitas" which is situated in the National Park Pan de Azúcar in the Southern Atacama Desert. Here, quartz- and granitoid grit-sized (6 mm) stones paved the desert surface. Blackish and whitish patterns could frequently be observed on the ground in the landscape that were caused by varying colonization rates of the grit stones (Figure 1a). The whitish spots were colonized by <10% of different small lichen thalli whereas blackish appearing grits were 90% coated by these lichen communities resulting in blackish pattern in the landscape. Wherever this saxicolous (living on stones) biocenosis was present, terrain surfaces were concatenated by organisms occurring on and between the grits and smaller-sized mineral particles (Figure 1b). Amounts of chlorophyll$_{a+b}$ were more than five times higher in blackish compared with the whitish grit parts (Table 1). Remote sensing techniques revealed that the area covered by both patterns in the Pan de Azúcar National Park was as large as 350 km^2 with coverages between 20% and 80% (Figure 1c). The biocenosis (Figure 2a,b) was dominated by a high number of chlorolichen species of the genus *Buellia* and more rarely *Pleopsidium*

TABLE 1 Climatic characterization of the study area, data from July 2017 to March 2018

Longitude	[°W; WGS84]	-70.61521111
Latitude	[°S; WGS84]	-25.96636111
PAR$_{mean}$	[μmol/m^2 s^{-1}]	892.72 ± 727.53
PAR$_{max}$	[μmol/m^2 s^{-1}]	2,596
MAT$_{ground/air}$ [a]	[°C]	15.5 ± 9.4/ 12.0 ± 3.3
Tmin$_{ground/air}$ [a]	[°C]	0.2/ 4.4
Tmax$_{ground/air}$ [a]	[°C]	41.8/ 24.6
MFWI$_{ground}$	[ml/m^2 day^{-1}]	125; average of 73% of all hours
MDWI	[ml/m^2 day^{-1}]	44; average of 4.9% of all hours

Note: Means and standard deviations of daily values in the case of PAR$_{max}$, T_{min}, and T_{max}.
Abbreviations: MAT, mean annual temperature; MDWI, mean dew water input; MFWI, mean fog water input; PAR, photosynthetic active radiation.
[a]2 m height.

chlorophanum and non-lichenized fungi of the genus *Lichenothelia* or relatives (Dothideomycetes) (Figure 2a white triangle, 2b). As detected by enrichment cultures, there were also free-living green algae species such as *Stichococcus deasonii* (Figure 2c), *Trebouxia*, *Apatococcus*, and *Chlorella* as well as cyanobacteria (reviewed in Jung et al., 2019) like the filamentous species *Microcoleus vaginatus* (Figure 2d), *Scytonema hyalinum*, the unicellular *Pleurocapsa minor*, and *Chroococcidiopsis* sp. found in the biocenosis of the CGC.

3.2 | Ecophysiology and environmental conditions

Climate records showed that dew occurred frequently, predominately during night-time providing between 0.025 and 0.088 mm of liquid water per day (Table 1, Figure 3a). In contrast to dew, fog usually occurred during daytime and provided higher water fluxes delivering 0.38–1.25 mm per day (Table 1). As such, the majority of the total water deposition (92%) was from fog, which mainly was deposited from morning till noon (Figure 3a). High irradiation, with maxima of more than 1,500 μmol photons/m^2 s^{-1}, was recorded during cloud-free periods (Table 1, Figure 3b). Mean annual temperatures (MAT) ranged between 12°C (air) and 15°C (ground level) (Table 1).

During gas exchange measurements in the laboratory, the optimum water content for photosynthesis of the CGC was found at 0.25 mm (Figure 3c). Besides that, we measured a high light compensation point (LCP; the light level where photosynthesis equals respiration), as well as a high light saturation point for photosynthesis (LSP, 90% of max. net photosynthesis (NP)) of 460 ± 29 and 1625 ± 112 μmol photons/m^2 s^{-1}, respectively (Table 2).

The maximum of NP of the CGC was reached at 10°C while an increase to 15 and 20°C had no effect on NP (Figure 3d). However, dark respiration (DR) strongly increased with raising temperatures, indicating that increasing gross photosynthesis did

compensate for additional respirational CO_2 release. Thus, optimal temperature regimes for net primary productivity are those of daytime temperatures above 10°C and night temperatures below 10°C (Figure 3d).

3.3 | Ecosystem services provided by the new biocrust type

Cross-sections of colonized grit stones revealed mycobiont hyphae penetrating the outer and inner grit-sized stones and photobionts affiliated by mycobiont hyphae inside the grit stones (Figure 4a). Thin sections of the lichens showed mineral fragments incorporated into the lichen's thalli (Figure 4b).

Elemental analyses on C, N, and P revealed that the blackish pattern contained over three times more organic C and N than the whitish pattern (Table 2). We extrapolated C, N, and P stocks (1.5 cm depth) to the area fully covered by the grit–crust. In total, the grit–crust stores approx. 266 tons of C in the National Park Pan de Azúcar (350 km^2) of which almost 250 tons are organic C. Stocks of N and P sum up to 27 tons and 68 tons, respectively. If the area of blackish pattern would be covered by the whitish pattern, total C and N stocks would be approx. 165 tons and 16 tons less, respectively.

Py-FIMS analyses revealed 47.3% of biocrust organic matter which was tentatively assignable to nine different compound classes. The contribution of the organic compound classes (in % TII) decreased in the order ALKYL (9.3)> PHLM (7.7)> CHYDR (7.1)> LIPSTERO (6.5)> FATTY (4.7)> PEPTI (4.6)> LDIM (3.9)> NCOMP (2.9)> SUBER (0.6) (Figure 3e). Calculations based on the thermogram disclosed a total thermostability of the CGC of 0.5 (Figure 3f).

4 | DISCUSSION

4.1 | Ecology of the novel biocenosis

The blackish patterns paving the ground on a large landscape scale in the fog oasis Las Lomitas in the Atacama Desert were caused by an intimate biocenosis made of fungi, pro-, and eukaryotic algae on grit-sized quartz and granitoid stones (locally called "*maicillo*"), that can be assigned to the CGCs as described by Elbert et al. (2012), in accordance with our first hypothesis. This CGC is a saxicolous biocenosis since the organisms almost exclusively colonize grit-sized stones. However, it far more resembles a biocrust (Belnap, Büdel, & Lange, 2001, 2003) due to its ability to concatenate the grit-sized stones and to thus form stabilized pavement on the ground. Further, the Regosols in the area were marked by the occurrence of a thin A horizon with very low soil organic matter contents (<0.4%) and a finer grain structure under the thin pavement of grit (Bernhard et al., 2018). This resembles an edaphic substrate rather than rock. For these reasons, we named this type of CGC "*grit-crust*" to imply the transitional form of this biocenosis between a soil crust and rock cover, due to its unique substrate. In contrast to known biocrust
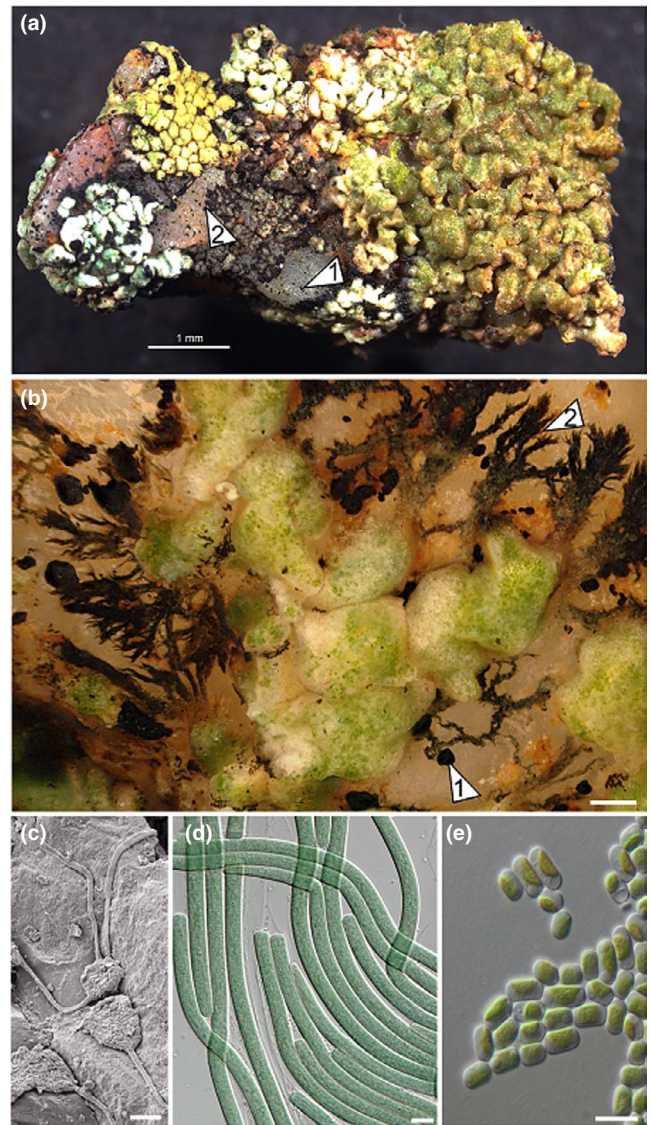
FIGURE 2 Grit-crust community. (a) Various hydrated lichens attached to two grit stones connecting them with *Lichenothelia* fungi (white triangle 1) and prothallus structures from the lichen (white triangle 2). (b) Closeup of single grit stone covered by hydrated lichens, with *Lichenothelia* sp. (white triangle 1) and prothalli of the lichens (white triangle 2), scale bar 200 μm. (c) Scanning electron microscopy of *Lichenothelia* sp. attached to the grit surface, scale bar 10 μm. (d) Light microscopy of the filamentous *cyanobacterium Microcoleus vaginatus* and the green algal species *Stichococcus deasonii* (e), scale bar 10 μm, each

types, such as pinnacled or flat biocrusts (Belnap, 2003), this new biocrust grew around grit stones covering them on all sides and concatenating them.

Various epiphytic and saxicolous lichens covering a large area in Pan de Azúcar were reported earlier (Follmann, 1965; Redon, 1973; Rundel, 1978; Rundel et al., 1991), while our results showed that the blackish pattern on the ground was caused by high colonization rates of the grit–crust that locally covered 80% of the desert surface as discovered by remote sensing techniques. With this, remote sensing
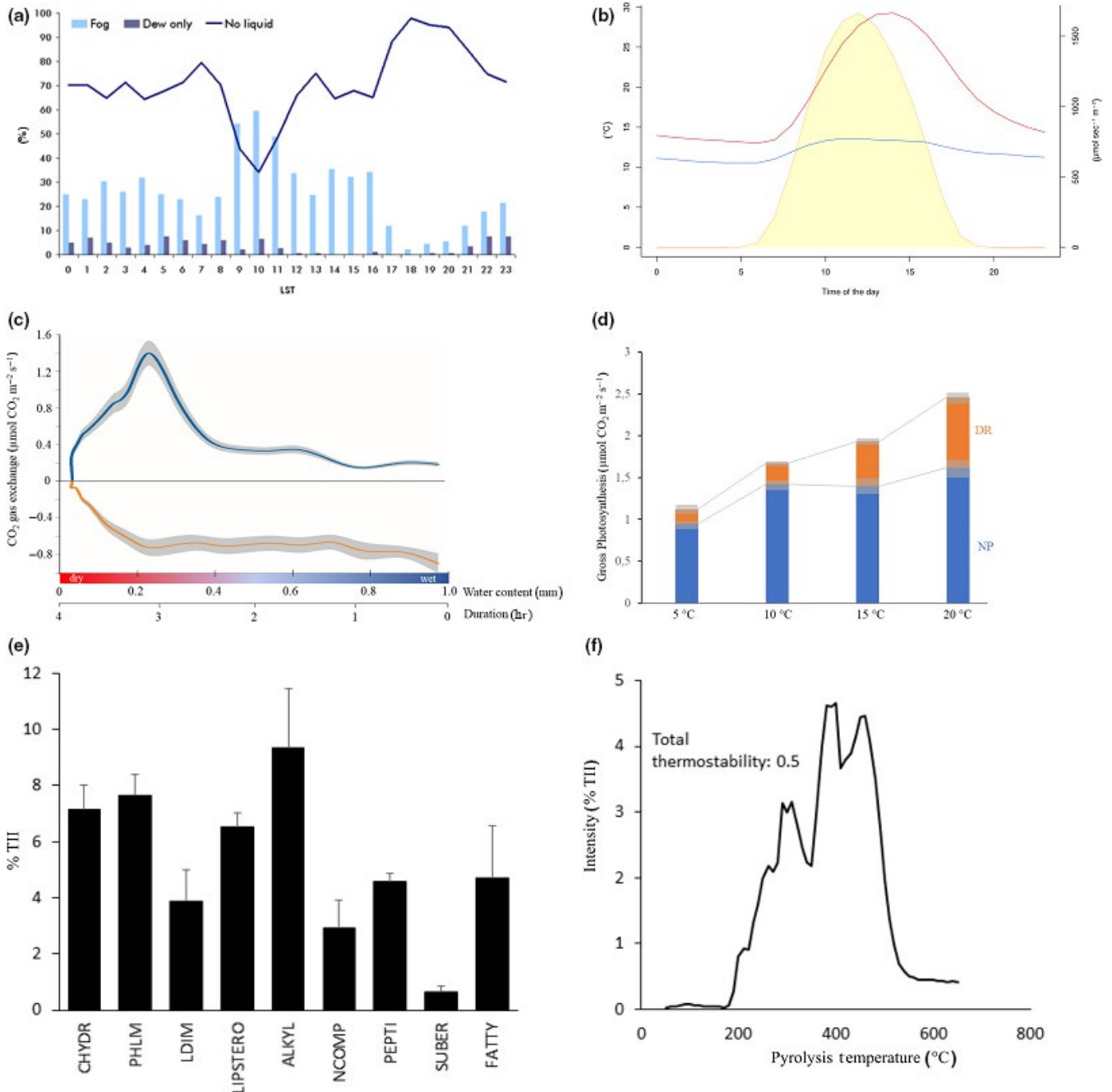
FIGURE 3 Climatic data, ecophysiology and chemistry. (a) Mean hourly frequency of fog and dew deposition showing the relative occurrence of fog and dew depositions recorded by the weather station at Las Lomitas over one year. Light blue bars indicate the average percentage of fog during a given hour of the day, whereas dark blue bars show the percentage of only dew during that hour. The blue line represents the percentage without any liquid supply during a particular hour. (b) average daily course of soil temperature (red), air temperature (blue), and photosynthetic active radiation (PAR; yellow), as the hourly averages of soil temperature (red), air temperature (blue), and PAR (yellow). (c) Mean CO_2 exchange of a grit-crust (blue represents net photosynthesis (NP), orange represents dark respiration (DR)) during desiccation at 15°C with respect to time (reverse axis) and water content (expressed as mm precipitation equivalent) and standard deviation in grey with $n = 5$. (d) Temperature dependence of photosynthesis and respiration as 90% of maximum values. Dark respiration (=DR, orange) represents C loss, net photosynthesis (=NP, blue) represents net C gain. Standard deviations are indicated in grey. (e) Organic compound classes (chemical profiling) of grit-crust community determined by Py-FIMS, given as percent of total ion intensity (TII), carbohydrates with pentose and hexose subunits (CHYDR), phenols and lignin monomers (PHLM), lignin dimers (LDIM), lipids, alkanes, alkenes, bound fatty acids, alkyl monoesters and sterols (LIPSTERO), alkylaromatics (ALKYL), mainly heterocyclic N-containing compounds (NCOMP), peptides (PEPTI), suberin (SUBR) and free fatty acids (FATTY). (f) Thermogram of total volatilization and calculated thermostability of the organic compounds of these compound classes in total organic compounds of the grit-crust community

TABLE 2 Chemical and ecophysiological characteristics of blackish and whitish patterns (0–0.9 cm depth) observed in the Coastal Atacama Desert of Chile

Parameter		Whitish pattern		Blackish pattern		p	Elemental stocks of blackish pattern [t 350 km^{-2}]
		Mean	±	Mean	±		
C_{total}	[g/m^2]	1.22	0.60	3.21	0.87	0.021*	266.47
$C_{inorganic}$	[g/m^2]	0.49	0.37	0.21	0.10	0.143	17.43
$C_{organic}$	[g/m^2]	0.73	0.39	3.00	0.78	0.008*	249.04
N	[g/m^2]	0.13	0.05	0.32	0.10	0.008*	26.56
S	[g/m^2]	0.24	0.04	0.21	0.03	0.458	17.43
P	[mg/m^2]	998.98	221.61	815.74	90.40	0.151	67.72
Chl_{a+b}	[mg/m^2]	25.87	3.72	138.19	17.41	0.008*	11.47
LSP	[μmol/m^2 s^{-1}]	–	–	1625	112		
LCP	[μmol/m^2 s^{-1}]	–	–	460	29		

Note: Given are means and standard deviations; n = 5; asterisks indicate significant differences of parameters between whitish and blackish pattern at $p ≤ .05$; Chl_{a+b} = Chlorophyll a + b.
Abbreviations: LCP = light compensation point of grit–crust photosynthesis; LSP = light saturation point.

techniques were successfully applied to detect desert biocrusts on a large landscape scale for the first time. Field observations showed that the distinct distribution of blackish and whitish patterns in the landscape might have been caused by windward and leeward exposure, respectively. In addition, this part of the Atacama Desert experiences infrequent rain events (Thompson, Palma, Knowles, & Holbrook, 2003) which are followed by the emergence of ephemeral herb cover (plants with a short life cycle). It will be interesting to study how this cover affects the performance and distribution of grit–crust organisms, as it temporarily changes the near-ground microclimate, reducing light levels and possibly dew formation, while increasing organic-matter inputs.

Similar blackish and whitish patterns in the landscape were reported from the lichen fields in the fog zone of Walvis Bay in the Namib Desert (Lange, Meyer, Zellner, et al., 1994) (Figure 1d). However, from Walvis Bay, which has a similar water regime as Las Lomitas, a biocrust of the grit–crust type is unknown so far. Only biocrusts dominated by the terricolous chlorolichen *Acarospora gypsidesertii* are reported (Büdel et al., 2009; Lange, Meyer, Zellner, et al., 1994). The easily overlooked grit–crust of Las Lomitas has not been explicitly searched for in other fog-influenced desert zones worldwide so far, so that it remains uncertain to what extent grit–crust-like biocrusts occur.

4.2 | Ecophysiology of the grit–crust community

The water regime at Las Lomitas facilitated mainly eukaryotic green algae and green-algal lichens to colonize the grit stones. Both types of organisms are known to be activated by liquid water sources (rainfall, fog, dew) and additionally by relative air humidity higher than 85% (Lange and Büdel 1994; Büdel, Vivas, & Lange, 2013). In contrast, cyanobacterial lichens (cyanolichens) and cyanobacteria can only be activated by liquid water (Büdel & Lange, 1991; Lange, Kilian, & Ziegler, 1986). Interestingly, in contrast to our second hypothesis, cyanobacteria were part of the grit–crust community as

well, probably because the two main liquid water sources, fog and dew, were frequently available at Las Lomitas (Lehnert, Thies, et al., 2018b). We noticed that cyanobacterial presence in the arid and hyperarid zone of the Atacama Desert (e.g., Warren-Rhodes et al., 2006, Wierzchos, Ascaso, & McKay, 2006) is apparently directly related to microhabitats that provide a condensation surface large enough for dew and fog to precipitate. This seems to provide a sufficient amount of liquid water for cyanobacteria to thrive.

To support and maintain its biological activity, the grit–crust community depends on achieving a positive net photosynthesis under strongly limiting moisture conditions. In the laboratory, the optimum water content for photosynthesis of the grit–crust community was 0.25 mm (Fig. 3c), which is a remarkably low amount of water, if compared to other biocrusts worldwide. In the fog zone of the Namib Desert, for example, biocrusts dominated by the lichen *Acarospora schleicheri* had their optimal water content at more than twice as much (6 mm) (Lange, Meyer, Zellner, et al., 1994), and other lichen-dominated biocrusts from the Sonora Desert had their optimal water content between 0.5 and 1 mm (Büdel et al., 2013). Thus, it can be deduced that the newly discovered grit–crust is well adapted to the arid conditions in the Atacama Desert, where water is solely available from fog and dew. The pronounced tolerance of the grit organisms against xeric stress has also been demonstrated for lichens such as *Pleopsidium chlorophanum* and *Buellia* species from Antarctica, which are reported to even acclimatize to Martian conditions (de Vera et al., 2014; Verseux et al., 2016), and which were both also found in the Las Lomitas grit–crust. Conditions in the Atacama Desert have indeed been compared to those on Mars and the very low water demands of the grit–crust community documented here supports the hypothesis (Verseux et al., 2016) about the extremophile character of these organisms, which may even be suitable candidates for extra-terrestrial colonization and may have played a role shaping soils and the atmosphere on the ancient Earth.
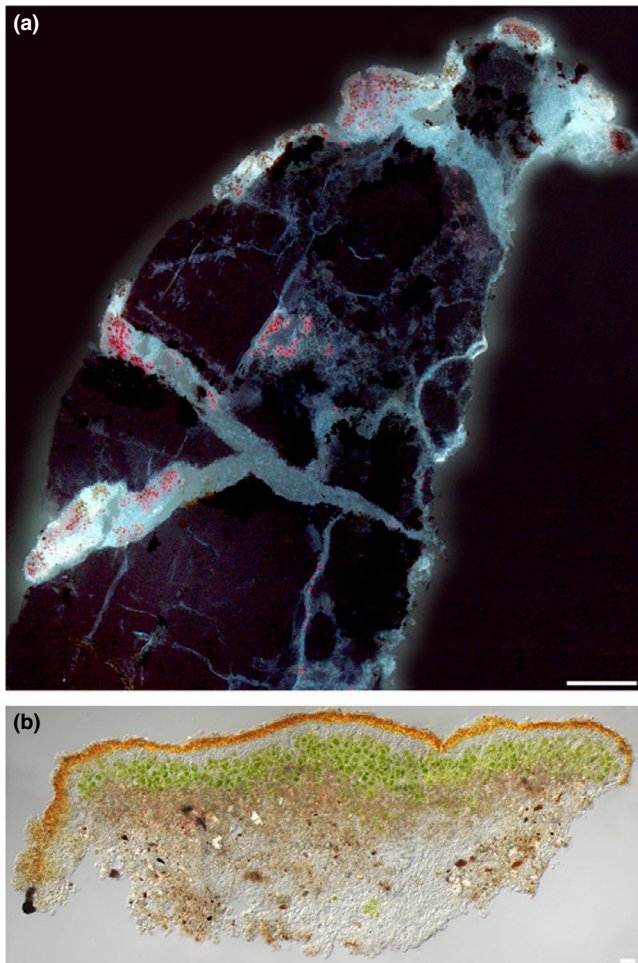
FIGURE 4 Indication of bio-weathering. (a) Fluorescence microscopy image of a thin section of a single grit which is penetrated by hyphae of lichens (white) together with their green algal photobionts (red), scale bar 1 mm. (b) Thin section of a lichen detached from the grit surface with mineral fragments incorporated into the lichen's thallus, scale bar 20 µm

Intensive solar radiation and high temperature in desert environments can also limit photosynthesis. During fog events radiation levels are low, but as soon as the fog clears intensive radiation might cause (i) a fast heating-up of the biocrust combined with a rapid desiccation that protects the photosynthetic apparatus from damages or (ii) photoinhibition during a slow heating process. As shown by its high LCP, however, the grit–crust was well adapted to high light intensities. Gas exchange measurements showed that the optimal temperatures for net primary productivity were above 10°C during the day, with no decrease in NP up to at least 20°C. Such conditions are provided with the average daily temperature course at this site (Figure 3b) (Baumann et al., 2018). Adaptation to fog–desert conditions requires an optimum photosynthetic activity during fog events where light can be quite low, temperatures are moderate, and sufficient liquid water is available but will quickly evaporate after the fog disappears. According to our measurements, optimal photosynthetic activity of the grit–crust

community can be expected in the morning hours, especially between 9 and 11 a.m. when light availability is good and water supply is warranted by dew and fog (Figure 3a,b). The diurnal cycle of fog and dew water fluxes demonstrated that the most critical hours for photosynthesis of the grit–crust can be expected in the afternoon, especially after 4 p.m., when liquid water supply by fog and dew is hardly available. A similar conclusion is supported by the climate data recorded by Thompson et al. (2003) over the course of three years for the same location. The fluctuating water regime at Las Lomitas causes frequent wet–dry cycles, which would be lethal for some biocrust types from arid zones without fog. For those biocrusts, such slight and almost daily slender wetting would cost more in recovery respiration than would be won by photosynthetic gain (Belnap, Phillips, & Miller, 2004; Reed et al., 2012). Therefore, the newly discovered grit–crust is quite unique in a way that every fog event can be seen as the *"desert's breath"* which is followed by instant biological activity such as primary production and other fundamental ecosystem services which are of high significance in poor ecosystems such as the Atacama Desert.

4.3 | Ecosystem services and the potential importance of cryptogams for the ancient Earth

Biocrusts have played an important role during the evolution of terrestrial ecosystems by mineral weathering and soil development since the Paleozoic (Mitchell et al., 2016). The occurrence of for example lichens as a symbiosis between algae and fungi dates back to the Precambrian 400 million years ago (Taylor & Osborn, 1996), while cyanobacteria are suspected to have played a significant role during early oxygen production and atmospheric enrichment with oxygen even before the Great Oxidation Event (GOE) 2.45–2.32 billion years ago (Lalonde & Konhauser, 2015; Schirrmeister, de Vos, Antonelli, & Bagheri, 2013). Until land plants appeared, about 70 million years ago (Heckman, Geiser, Eidell, Stauffer, Kardos, & Hedges, 2001), the terrestrial organic C pool of early soils as well as the atmospheric oxygen pool was fueled solely by the biological activity of cryptogams for a long geological period (Lalonde & Konhauser, 2015; Mergelov et al., 2018). Assuming that the arid to hyperarid conditions of the Atacama Desert have been stable since the middle Miocene (Sun, Bao, Reich, & Hemming, 2018), the grit–crust community found at the modern coastal Atacama could be a continuation of a very early community type. As a consequence, the grit–crust could act as a model community which fixes C during photosynthesis, conducts bio-weathering processes, and releases oxygen in the same way it may have since before the emergence of land plants (Makeev, 2015; Mergelov et al., 2018; Retallack, 2001).

For example cyanobacteria detected in the recent grit–crust, promote bio-weathering by causing alkaline conditions which can dissolve quartz. This has been demonstrated for the cyanobacterium *Chroococcidiopsis* (Büdel et al., 2004), which is one of the genera found in the grit–crust community. In addition to bio-weathering activity via alkalization, we also found mechanical bio-weathering by contraction

and expansion of lichen thalli during the wet–dry cycles. This causes cracks within the stones (Figure 4a) which is known to contribute to bioweathering (Chen, Blume, & Beyer, 2000) and, finally, to initial soil formation. In addition to lichens and cyanobacteria, also the fungal genus *Lichenothelia* was part of the grit–crust community and is known to also grow on and within exposed rocks in the Sonoran and Mojave Desert contributing to bio-weathering in the same way as lichens (Muggia, Kocourková, & Knudsen, 2015). Besides mineral breakdown by the grit–crust organisms, the desert surface is transformed into initial soils by C and N input from the biocrust (Table 2) influencing geomorphological processes from the micro- to the landscape scale. As Py-FIMS analyses revealed, the grit–crust community and thus the potential input of organic C from the grit–crust consisted of 11.5% phenolic derivates followed by 9.3% alkyl aromatic compounds. These substance classes are not just relatively heat resistant but also relatively difficult to decompose and are known to accumulate, for example, in steppe-like environments (Leinweber et al., 2009). We conclude that accumulation processes lead to the formation of a *terrestrial protopedon* with a cryptic A horizon enriched in C and N, as suspected in our third hypothesis. Similar processes of soil formation were reported for Antarctica (Mergelov et al., 2018), where cyanobacteria and fungi contributed to the formation of soils. This could be a significant contribution to biogeochemical cycles in such organic matter poor desert environments and even to global cycles if we assume that large areas in fog-influenced deserts may be covered by similar but, to date, undiscovered biocrust types. Although probably slow growing and not being a large pool of C and N, the new grit–crust type is still the one and only transformer of the desert's mineral substrate into an early type of soil (protopedon) that we are aware of for a considerable part of the Atacama Desert.

5 | CONCLUSIONS

We conclude that the grit–crust is the primary supporter of the poor desert ecosystem with its few and highly scattered vascular plants and a hitherto unknown or only partly known contingent of heterotrophic bacteria, microfungi, protists, invertebrates, and the better-known small vertebrates and finally larger mammals like foxes and guanacos. Additionally, this biocenosis might be highly comparable to communities shaping ancient Earth. For both of these reasons, this highly interesting and widespread grit–crust ecosystem certainly deserves more research to better understand its full taxonomic composition and the ecophysiological traits that guarantee activity and survival. Additional multidisciplinary surveys are recommended in the Atacama and other deserts globally, to extend our knowledge of the functioning of this newly discovered biocrust type and its contribution to these unique ecosystems.

CONFLICT OF INTEREST

The authors declare that they have no conflict of interest.

AUTHOR CONTRIBUTION

PJ, BB, KB, LL, and JB conceived the study; LL, SA, and LW collected and calculated the remote sensing data; PJ, MS, and BB conducted the ecophysiological experiments and identified together with ES the organisms, KB analyzed the soil parameters of the samples and KUE conducted the Py-FIMS analyses. PJ wrote the manuscript with input and editing from MB, JB, UK, PL, and BB and all other coauthors.

ORCID

Patrick Jung https://orcid.org/0000-0002-7607-3906
Maaike Y. Bader https://orcid.org/0000-0003-4300-7598
Ulf Karsten https://orcid.org/0000-0002-2955-0757
Jörg Bendix https://orcid.org/0000-0001-6559-2033

REFERENCES

Baumann, K., Jung, P., Samolov, E., Lehnert, L. W., Büdel, B., Karsten, U., … Leinweber, P. (2018). Biological soil crusts along a climatic gradient in Chile: Richness and imprints of phototrophic microorganisms in phosphorus biogeochemical cycling. *Soil Biology & Biochemistry*, *127*, 286–300.

Belnap, J. (2003). The world at your feet: Desert biological soil crusts. *Frontiers in Ecology and the Environment*, *1*(4), 181–189.

Belnap, J., Büdel, B., & Lange, O. L. (2001, 2003).Biological soil crust: characteristics and distribution. In J. Belnap, & O. L. Lange (Eds.), *Biological soil crusts: Structure, Function, and Management. Ecological Studies*, *150*, 3–30.

Belnap, J., & Gardner, J. S. (1993). Soil microstructure in soils ofthe Colorado Plateau: The role of the cyanobacterium Microcoleus vaginatus. *Great Basin Naturalist*, *53*, 40–47.

Belnap, J., Phillips, S. L., & Miller, M. E. (2004). Response of desert biological soil crusts to alterations in precipitation frequency. *Oecologia*, *141*(2), 306–316. https://doi.org/10.1007/s00442-003-1438-6

Bernhard, N., Moskwa, L. M., Schmidt, K., Oeser, R. A., Aburto, F., Bader, M. Y., …Brucker, E. (2018). Pedogenic and microbial interrelations to regional climate and local topography: New insights from a climate gradient (arid to humid) along the Coastal Cordillera of Chile. *Catena*, *170*, 335–355.

Bischof, H., Bold, H., & Studies, I. V. (1963). Some Soil Algae from enchanted rock and related algal species (Vol. *6318*, pp. 1–95) :Austin, TX: University of Texas Publication.

Blume, H. P., Stahr, K., & Leinweber, P. (2010). *Bodenkundliches Praktikum, 3. Auflage* (p. 255). Heidelberg, Germany: Spektrum Akademischer Verlag.

Bowker, M. A., Mau, R. L., Maestre, F. T., Escolar, C., & Castillo-Monroy, A. P. (2011). Functional profiles reveal unique ecological roles of various biological soil crust organisms. *Functional Ecology*, *25*(4), 787–795. https://doi.org/10.1111/j.1365-2435.2011.01835.x

Büdel, B., Darienko, T., Deutschewitz, K., Dojani, S., Friedl, T., Mohr, K. I., ... Weber, B. (2009). African biological soil crusts are ubiquitous and highly diverse in drylands, being restricted by rainfall frequency. *Microbial Ecology*, 57(2), 229–247. https://doi.org/10.1007/s00248-008-9449-9

Büdel, B., & Lange, O. L. (1991). Water status of green and blue-green phycobionts in lichen thalli after hydration by water vapor uptake: Do they become turgid? *Botanica Acta*, 104, 361–366.

Büdel, B., Vivas, M., & Lange, O. L. (2013). Lichen species dominance and the resulting photosynthetic behavior of Sonoran Desert soil crust types (Baja California, Mexico). *Ecological Processes*, 2(1), 6. https://doi.org/10.1186/2192-1709-2-6

Büdel, B., Weber, B., Kühl, M., Pfanz, H., Sültemeyer, D., & Wessels, D. (2004). Reshaping of sandstone surfaces by cryptoendolithic cyanobacteria: Bioalkalization causes chemical weathering in arid landscapes. *Geobiology*, 2(4), 261–268. https://doi.org/10.1111/j.1472-4677.2004.00040.x

Chen, J., Blume, H. P., & Beyer, L. (2000). Weathering of rocks induced by lichen colonization—a review. *Catena*, 39(2), 121–146. https://doi.org/10.1016/S0341-8162(99)00085-5

Chen, M., & Ma, L. Q. (2001). Comparison of three aqua regia digestion methods for twenty Florida soils. *Soil Science Society of America Journal*, 65(2), 491–499. https://doi.org/10.2136/sssaj2001.652491x

Curatola Fernández, G. F., Obermeier, W. A., Gerique, A., Sandoval, M. F. L., Lehnert, L. W., Thies, B., & Bendix, J. L. (2015). Cover Change in the Andes of Southern Ecuador - Patterns and Drivers. *Remote Sensing*, 7, 2509–2542.

de Vera, J. P., Schulze-Makuch, D., Khan, A., Lorek, A., Koncz, A., Möhlmann, D., & Spohn, T. (2014). Adaptation of an Antarctic lichen to Martian niche conditions can occur within 34 days. *Planetary Space Sciences*, 98, 182–190. https://doi.org/10.1016/j.pss.2013.07.014

Drees, K. P., Neilson, J. W., Betancourt, J. L., Quade, J., Henderson, D. A., Pryor, B. M., & Maier, R. M. (2006). Bacterial community structure in the hyperarid core of the Atacama Desert, Chile. *Applied and Environmental Microbiology*, 72(12), 7902–7908. https://doi.org/10.1128/AEM.01305-06

Elbert, W., Weber, B., Burrows, S., Steinkamp, J., Büdel, B., Andreae, M. O., & Pöschl, U. (2012). Contribution of cryptogamic covers to the global cycles of carbon and nitrogen. *Nature Geoscience*, 5, 459–462. https://doi.org/10.1038/ngeo1486

Evans, R. D., Koyama, A., Sonderegger, D. L., Charlet, T. N., Newingham, B. A., Fenstermaker, L. F., ... Nowak, R. S. (2014). Greater ecosystem carbon in the mojave desert after ten years exposure to elevated CO_2. *Nature Climate Change*, 4(5), 394. https://doi.org/10.1038/nclimate2184

Follmann, G. (1965). Eine gesteinsbewohnende Flechtengesellschaft der nordchilenische Wüstenformationen mit kennzeichnender *Buellia albula* (Nyl.) Muell.-Arg. *Nova Hewigia*, 10, 243–256.

Hartley, A. J., Chong, G., Houston, J., & Mather, A. E. (2005). 150 million years of climatic stability: Evidence from the Atacama Desert, northern Chile. *Journal of the Geological Society*, 162(3), 421–424.

Heckman, D. S., Geiser, D. M., Eidell, B. R., Stauffer, R. L., Kardos, N. L., & Hedges, S. B. (2001). Molecular evidence for the early colonization of land by fungi and plants. *Science*, 293(5532), 1129–1133.

Jung, P., Schermer, M., Briegel-Williams, L., Baumann, K., Leinweber, P., Karsten, U., ... Büdel, B. (2019). Water availability shapes edaphic and lithic cyanobacterial communities in the Atacama Desert. *Journal of Phycology*. https://doi.org/10.1111/jpy.12908

Lalonde, S. V., & Konhauser, K. O. (2015). Benthic perspective on Earth's oldest evidence for oxygenic photosynthesis. *Proceedings of the National Academy of Sciences*, 112(4), 995–1000.

Lange, O. L., Kilian, E., & Ziegler, H. (1986). Water vapor uptake and photosynthesis of lichens: Performance differences in species with green and blue-green algae as phycobionts. *Oecologia*, 71, 104–110.

Lange, O. L., Meyer, A., & Büdel, B. (1994). Net-photosynthesis of a desiccated cyanobacterium without liquid water in high air humidity alone. Experiments with *Microcoelus sociatus* isolated from a desert soil crust. *Functional Ecology*, 8, 52–57.

Lange, O. L., Meyer, A., Zellner, H., & Heber, U. (1994). Photosynthesis and water relations of lichen soil crusts: Field measurements in the coastal fog zone of the Namib Desert. *Functional Ecology*, 8(2), 253–264.

Lehnert, L., Jung, P., Obermeier, W., Büdel, B., & Bendix, J. (2018a). Estimating net photosynthesis of biological soil crusts in the Atacama using hyperspectral remote sensing. *Remote Sensing*, 10(6), 891.

Lehnert, L. W., Thies, B., Trachte, K., Achilles, S., Osses, P., Baumann, K., ... Bendix, J. (2018b). A case study on fog/low stratus occurrence at Las Lomitas, Atacama Desert (Chile) as a water source for biological soil crusts. *Aerosol and Air Quality Research*, 18, 254–269.

Leinweber, P., Jandl, G., Eckhardt, K.-U., Schulten, H.-R., Schlichting, A., & Hofmann, D. (2009). Analytical pyrolysis and soft-ionization mass spectrometry. In N. Senese, X. Boashan, & P. M. Huang (Eds.), *Biophysico-chemical processes involving natural nonliving organic matter in environmental systems* (pp. 539–588). New York, NY: Wiley.

Ma, J., Liu, R., Tang, L.-S., Lan, Z.-D., & Li, Y. (2014). A Downward CO_2 flux seems to have nowhere to go. *Biogeosciences*, 11(22), 6251–6262.

Maestre, F. T., Escolar, C., de Guevara, M. L., Quero, J. L., Lázaro, R., Delgado-Baquerizo, M., ... Gallardo, A. (2013). Changes in biocrust cover drive carbon cycle responses to climate change in drylands. *Global Change Biology*, 19(12), 3835–3847. https://doi.org/10.1111/gcb.12306

Makeev, A. O. (2015). Theory, diversity of natural evolution and anthropogenic transformations of soils. In I. V. Ivanov, & V. N. Kudeyarov (Eds.), *Evolution of soils and soil cover* (Ch. 9, pp. 253–320). (Geos, Moscow, 2015).

McKay, C. P., Friedmann, E. I., Gómez-Silva, B., Cáceres-Villanueva, L., Andersen, D. T., & Landheim, R. (2003). Temperature and moisture conditions for life in the extreme arid region of the Atacama Desert: Four years of observations including the El Niño of 1997–1998. *Astrobiology*, 3(2), 393–406.

Mergelov, N., Mueller, C. W., Prater, I., Shorkunov, I., Dolgikh, A., Zazovskaya, E., ... Goryachkin, S. (2018). Alteration of rocks by endolithic organisms is one of the pathways for the beginning of soils on Earth. *Scientific Reports*, 8(1), 3367. https://doi.org/10.1038/s41598-018-21682-6

Mitchell, R. L., Cuadros, J., Duckett, J. G., Pressel, S., Mavris, C., Sykes, D., ... Kenrick, P. (2016). Mineral weathering and soil development in the earliest land plant ecosystems. *Geology*, 44(12), 1007–1010. https://doi.org/10.1130/G38449.1

Muggia, L., Kocourková, J., & Knudsen, K. (2015). Disentangling the complex of Lichenothelia species from rock communities in the desert. *Mycologia*, 107(6), 1233–1253. https://doi.org/10.3852/15-021

Navarro-González, R., Rainey, F. A., Molina, P., Bagaley, D. R., Hollen, B. J., de la Rosa, J., ... McKay, C. P. (2003). Mars-like soils in the Atacama Desert, Chile, and the dry limit of microbial life. *Science*, 302, 1018–1021. https://doi.org/10.1126/science.1089143

Quéré, C. L., Andrew, R. M., Friedlingstein, P., Sitch, S., Hauck, J., Pongratz, J., ... Zheng, B. (2018). Global Carbon Budget 2018. *Earth System Science Data*, 10 (4): 2141–2194.

R Core Team. (2017). *R: A language and environment for statistical computing*. Vienna, Austria: R Foundation for Statistical Computing. https://www.R-project.org/

Redon, J. (1973). Beobachtungen zur Geographie und Okologie derchilenischen Flechtenflora. *Journal of the Hattori Botanical Laboratory*, 37, 153e167.

Reed, S. C., Coe, K. K., Sparks, J. P., Housman, D. C., Zelikova, T. J., & Belnap, J. (2012). Changes to dryland rainfall result in rapid moss mortality and altered soil fertility. *Nature Climate Change*, 2(10), 752. https://doi.org/10.1038/nclimate1596

Retallack, G. J. (2001). *Soils of the past: An introduction to paleopedology*. Oxford, UK: Blackwell Science.

Riano, D., Chuvieco, E., Salas, J., & Aguado, I. (2003). Assessment of different topographic corrections in Landsat-TM data for mapping vegetation types. *IEEE Transactions on Geoscience and Remote*, *41*, 1056–1061.

Rodriguez-Caballero, E., Belnap, J., Büdel, B., Crutzen, P. J., Andreae, M. O., Pöschl, U., & Weber, B. (2018). Dryland photoautotrophic soil surface communities endangered by global change. *Nature Geosci.*, *11*, 185–189. https://doi.org/10.1038/s41561-018-0072-1

Ronen, R., & Galun, M. (1984). Pigment extraction from lichens with dimethyl sulfoxide (DMSO) and estimation of chlorophyll degradation. *Environmental and Experimental Botany*, *24*(3), 239–245. https://doi.org/10.1016/0098-8472(84)90004-2

Rundel, P. W. (1978). Ecological relationships of desert fog zone lichens. *Bryologist*, *81*(2), 277–293. https://doi.org/10.2307/3242189

Rundel, P. W., Dillon, M. O., Palma, B., Mooney, H. A., Gulmon, S. L., & Ehleringer, J. R. (1991). The phytogeography and ecology of the coastal Atacama and Peruvian deserts. *Aliso: A Journal of Systematic and Evolutionary Botany*, *13*(1), 1–49.

Rundel, P. W., Villagra, P. E., Dillon, M. O., Roig-Juñent, S., & Debandi, G. (2007). Physical Geography of South America.In T. T. Veblen, K. R. Young, & A. R. Orme (Eds.), *Arid and semi-arid ecosystems* (pp. 158–183). Oxford, UK: Oxford University Press.

Schirrmeister, B. E., de Vos, J. M., Antonelli, A., & Bagheri, H. C. (2013). Evolution of multicellularity coincided with increased diversification of cyanobacteria and the Great Oxidation Event. *Proceedings of the National Academy of Sciences*, *110*(5), 1791–1796.

Schulten, H.-R., & Leinweber, P. (1999). Thermal stability and composition of mineral-bound organic matter in density fractions of soil. *European Journal of Soil Science*, *50*, 237–248. https://doi.org/10.1046/j.1365-2389.1999.00241.x

Selby, M. J. (1977). On the origin of sheeting and laminae in granitic rocks: Evidence from Antarctica, the Namib Desert and the Central Sahara. *Madoqua*, *1977*(v10i3), 171–179.

Stanier, R. Y., Kunisawa, R., Mandel, M., & Cohen-Bazire, G. (1971). Purification and properties of unicellular blue-green algae (order Chroococcales). *Bacteriological Reviews*, *35*, 171.

Sun, T., Bao, H., Reich, M., & Hemming, S. R. (2018). More than ten million years of hyper-aridity recorded in the Atacama Gravels. *Geochimica Et Cosmochimica Acta*, *227*, 123–132. https://doi.org/10.1016/j.gca.2018.02.021

Taylor, T. N., & Osborn, J. M. (1996). The importance of fungi in shaping the paleoecosystem. *Review of Palaeobotany and Palynology*, *90*(3-4), 249–262.

Thompson, M. V., Palma, B., Knowles, J. T., & Holbrook, N. M. (2003). Multi-annual climate in Parque Nacional Pan de Azúcar, Atacama Desert, Chile. *Revista Chilena De Historia Natural*, *76*, 235–254.

Vermote, E. F., Tanre, D., Deuze, J. L., Herman, M., & Morcette, J. J. (1997). Second simulation of the satellite signal in the solar spectrum, 6S: An overview. *IEEE Transactions on Geoscience and Remote Sensing*, *35*, 675–686. https://doi.org/10.1109/36.581987

Verseux, C., Baqué, M., Lehto, K., de Vera, J. P. P., Rothschild, L. J., & Billi, D. (2016). Sustainable life support on Mars–the potential roles of cyanobacteria. *International Journal of Astrobiology*, *15*(1), 65–92. https://doi.org/10.1017/S147355041500021X

Wang, F., Michalski, G., Luo, H., & Caffee, M. (2017). Role of biological soil crusts in affecting soil evolution and salt geochemistry in hyperarid Atacama Desert, Chile. *Geoderma*, *307*, 54–64. https://doi.org/10.1016/j.geoderma.2017.07.035

Warren-Rhodes, K. A., Rhodes, K. L., Pointing, S. B., Ewing, S. A., Lacap, D. C., Gómez-Silva, B., … McKay, C. P. (2006). Hypolithic cyanobacteria, dry limit of photosynthesis, and microbial ecology in the hyperarid Atacama Desert. *Microbial Ecology*, *52*(3), 389–398. https://doi.org/10.1007/s00248-006-9055-7

Weber, B., Büdel, B., & Belnap, J. (Eds.) (2016). *Biological soil crusts: An organizing principle in drylands*, Vol. *226*. Cham, Switzerland: Springer.

Wierzchos, J., Ascaso, C., & McKay, C. P. (2006). Endolithic cyanobacteria in halite rocks from the hyperarid core of the Atacama Desert. *Astrobiology*, *6*(3), 415–422. https://doi.org/10.1089/ast.2006.6.415